Extended Methods

RNA extraction from tissue

Skin tissue was homogenized in lysis buffer with Minilys by Bertin Technologies with 30sec homogenizing/30sec break cycle for a total of 3 cycles until tissue was completely disrupted. Alternatively, tissue was homogenized in Trizol (Thermo Fisher Scientific) using a tissue disruptor probe for 3 cycles of 30s pulses. Homogenates were processed for RNA extraction with Qiagen RNeasy Fibrous Tissue kit according to the manufacturer's protocol. RNA concentration was assessed using a spectrophotometer (NanoDrop).

RNA sequencing

Skin biopsies of three different cohorts were used for RNA sequencing analysis (Cohort 1, PRESS and cohort 3). Total RNA was fractionated to purify mRNA using the Dynabeads mRNA Purification Kit (Thermo Fisher Scientific) to minimize contamination from rRNA. Purified polyA mRNA was used as the template for reverse transcription. After first strand complementary DNA (cDNA) synthesis, the entire single strand cDNA was used for the double strand cDNA synthesis. The MinElute PCR Purification Kit (Qiagen) was used to concentrate the cDNA, and size selection of 200-300bp cDNA was carried out on an agarose gel. Illumina sequencing libraries were generated for the cDNA according to the manufacturer's sample preparation protocol, and then sequenced on the HiSeq2000 platform to generate paired 100bp long reads. Sequence reads was mapped to human genome using Bowtie and then processed with the software package TopHat and Cufflinks. The number of read counts per gene was estimated using HTseq. Differential expression analysis was carried out on variance stabilized counts using DEseq2 package 44 (Bioconductor, https://www.bioconductor.org/). In addition, clustering and principal component analyses were performed to screen for technical artefacts related to the date of sample collection, extraction and sequencing. These analyses did not indicate any batch effect. For the PRESS cohort similar procedures were pursued with the difference that a ribosomal reduction instead of poly (A) enrichment method was carried out. Specifically, cDNA libraries were prepared using the TruSeq Stranded Total RNA with Ribo-Zero Gold Kit (Illumina). Moreover, 2X 76 bp paired-end sequencing on HiSeq 2500 (Illumina) was conducted, generating approximately 50 million reads per sample. RNA sequencing performed on the skin biopsies from cohort 3 has been described recently (1).

Protein coding capacity

The LncRNA protein coding capacity was evaluated with the CPAT (http://rna-cpat.sourceforge.net/) analysis which is based on four pure sequence-based, linguistic features, ORF size, ORF coverage, Fickett TESTCODE and Hexamer usage bias. Analysis was done using default settings for human sequences, and coding probabilities below 0.364 were considered noncoding as described (2,3).

Cells and cell culture

Human pulmonary artery smooth muscle cells (HPASMC) were purchased from ScienCell and cultured in smooth muscle cell medium (SMCM, ScienCell) supplemented with 1% FBS, 100 units/ml of penicillin, 100 µg/ml of streptomycin and smooth muscle cell growth supplement (all ScienCell). Rheumatoid arthritis synovial fibroblasts (RASFs) were isolated from synovial tissues digested with dispase (37 °C, 1 h) and cultured in DMEM (Sigma-Aldrich) supplemented Penicillin and 50 µg/ml Streptomycin (Gibco) and 10% fetal bovine serum (10% FBS, Gibco), 2 mM L-glutamine, 10 mM HEPES and 0.2% amphotericin B (all from Life Technologies). BJ5TA hTERT-immortalized foreskin fibroblast cell line was purchased from ATCC and kept in medium constituted of four parts of DMEM (Sigma-Aldrich) and one part of Medium 199 (Sigma-Aldrich) supplemented with 0.01mg/ml hygromycin B (Sigma-Aldrich), 10% fetal bovine serum (10% FBS, Gibco), 50 U/ml Penicillin and 50µg/ml Streptomycin (Gibco). Human dermal microvascular endothelial cells (HDMEC) were purchased from ScienCell and cultured in endothelial cell medium (SMCM, ScienCell). CD14+ cells were isolated from blood of SSc patients using CD14 Microbeads (MACS, Miltenyi Biotec) according to the manufacturer's protocol and cultured in DMEM (Sigma-Aldrich) containing 50 U/ml Penicillin and 50 µg/ml Streptomycin (Gibco) and 10% fetal bovine serum (10% FBS, Gibco) and 100 µM 2-mercaptoethanol (Gibco). Purity was confirmed to be >95% by FACS analysis. Primary human keratinocytes (HK) were isolated from healthy skin derived from donors undergoing plastic surgery as previously described (4). Keratinocytes were maintained in keratinocyte-serum-free medium (KSF-M, Gibco) supplied with epidermal growth factor (EGF, Gibco) and Bovine Pituitary Extract (BPE, Gibco). All cell types were maintained in 5% CO2 humid 37°C incubator.

Cytokines and Inhibitors

For stimulation experiments, starvation medium (1% FBS) was supplemented either with 0.1-10ng/ml TGFβ (Peprotech), 20ng/ml PDGF (Peprotech), 10ng/ml IL-1β (ImmunoTools), 10ng/ml IL-4 (ImmunoTools), 10ng/ml IL-13 (ImmunoTools) or 10ng/ml IL-17a (ImmunoTools) for 6, 24 or 72h. TGFβR1 was blocked using 100nM SD208 inhibitor (Tocris) and 10µM SB431542 inhibitor (Tocris) in parallel to TGFβ treatment. Cells were starved for 24h prior to stimulation.

RNA extraction from cells

Total RNA from cells was isolated with Zymo Quick-RNA MicroPrep RNA isolation kit. RNA concentration was assessed using a spectrophotometer (NanoDrop).

Microarray

Two-hundred ng of total RNA was amplified and purified using a TotalPrep RNA Amplification Kit (Applied Biosystems/Ambion). Reverse transcription for first strand cDNA was performed using a T7 Oligo(dT) Primer to synthesize cDNA containing a T7 promoter sequence. Single stranded cDNA was then converted into double stranded cDNA and purified. In vitro transcription was used to amplify and label multiple copies of biotinylated cRNA. The amplified cRNA was hybridized on Illumina HT-12 arrays. The R-package 'lumi' was used to read and process the microarray raw data. For differential expression analysis was performed using 'limma' (5). The annotation is based on the R-package 'illuminaHumanv4.db'.

Reverse transcription-quantitative polymerase chain reaction (RT-qPCR)

One hundred twenty-five ng of RNA and random hexamers were used to carry out reverse transcription using the Transcriptor First Strand cDNA Synthesis kit (Roche). Subsequent qPCRs were performed with 2x SYBR Green master mix (Promega) on an Agilent Technologies Stratagene Mx3005P qPCR system. Ribosomal protein lateral stalk subunit P0 (*RPLP0*) and Glyceraldehyde 3-phosphate dehydrogenase (*GAPDH*) were used as reference housekeeping genes. Primer list is provided in Supplementary Table 7.

To analyze the expression of microRNAs, 10ng of RNA were reverse-transcribed using TaqMan MicroRNA Reverse Transcription Kit (Thermo Fisher Scientific) and pre-designed loop specific primers for miR-424 and miR-503 (Assay ID: 000604, 001048, Thermo Fisher Scientific). Pre-designed single TaqMan miRNA assays (Assay ID: 000604, 001048, Thermo Fisher Scientific) and TaqMan Universal Master Mix II, no UNG (Thermo Fisher Scientific) were used to measure the expression levels of miR-424 and miR-503. Expression of U48 small nucleolar RNA (RNU48) was used as endogenous control (Assay ID: 001006, Thermo Fisher Scientific).

Murine models

For bleomycin induced fibrosis, female 8 week old C57Bl6/J mice (Janvier, Le Genest-Saint-Isle, France) were injected intradermally every other day with either 100 bleomycin (0.5-1 mg/ml) or the vehicle NaCl (0.9%) (6) for 4 weeks. Lung fibrosis was induced in female 8 week old C57Bl6/J mice (Janvier, Le Genest-Saint-Isle, France) using intratracheally instilled bleomycin sulfate (Baxter, Kantonsapotheke Zurich, Switzerland) at a dosage of 4-2 U/kg of body weight (7). Control mice received equivalent volumes (50 µl) of 0.9% NaCl solution. For AdTGFβR1-induced fibrosis, 12-week-old mice (C57BL/6 background, Janvier, Le Genest-Saint-Isle,

France, mixed genders) received of 6.67 × 107 pfu/mouse of replication-deficient type 5 adenoviruses encoding for constitutively active TGFβR1 into marked areas of the upper back every other week for two months. Injections of replication-deficient type 5 adenoviruses encoding for *LacZ* were used as controls (8). TSK-1 mice (10 weeks of age, mixed genders) were interbred with pa/pa mice (The Jackson Laboratory, Bar Harbor, ME, USA).TSK-1 mice spontaneously develop increased dermal and hypodermal thickness as result of a partial in-frame duplication in the fibrillin-1 gene.

Bioinformatics analysis for ATAC-seq and ChIRP data

Data analysis for ChIRP-seq and ATAC-seq experiments was performed using the data analysis framework SUSHI (9). The raw reads were first cleaned by removing adapter sequences, trimming low quality ends, and filtering reads with low quality (phred quality <20) using Trimmomatic (10). Sequence alignment of the resulting high-quality reads to the Human genome (build GRCh38) was performed using Bowtie2 (Version 2.3.2) (11) with non-default options for the ATAC-Seq data: --no-mixed --no-discordant --very-sensitive -X 1500. For peak calling we used MACS2 (12). The resulting peaks were merged using Bedtools. The peak annotation to the closest transcription start site (TSS) was performed with the R-package ChIPpeakAnno using Ensembl's gene models of release 91 downloaded on February 26, 2018. The count values were computed with the function featureCounts from the R package R subread. Differential Count analysis was performed with the software package EdgeR (13).

Database search

WashU Epigenome Browser (http://epigenomegateway.wustl.edu/browser/) was used to navigate chromatin immunoprecipitation with sequencing (ChIP-seq) data for histone 3 lysine 27 acetylation (H3K27ac) and histone 3 lysine 4 mono-methylation (H3K4me1) performed in primary human dermal fibroblast. ChIP-seq data visualized with WashU Epigenome Browser (14) derived from other large consortia such as ENCyclopedia Of DNA Elements (ENCODE) (15). University of California Santa Cruz (UCSC) Genome Browser (https://genome.ucsc.edu/cgi-bin/hgGateway) (16) was used to navigate Ensembl Regulatory Build (17) data for DNA regulatory elements specific for primary human dermal fibroblast or fibroblast cell line (IMR90). UCSC Genome Browser was also used to access GeneHancer (18) database and predict gene-enhancer interactions, specifically 3D Genome Browser (http://promoter.bx.psu.edu/hi-c/index.html) (19) was used to visualize chromatin interaction data in the IMR90 cells obtained from Hi-C experiments (20).

References

1. Messemaker TC, Chadli L, Cai G, et al. Antisense Long Non-Coding RNAs Are Deregulated in Skin Tissue of Patients with Systemic Sclerosis. *J Invest Dermatol*. 2018;138(4):826-835.
2. Fickett JW. Recognition of protein coding regions in DNA sequences. *Nucleic Acids Res*. 1982;10(17):5303-5318.
3. Fickett JW, Tung CS. Assessment of protein coding measures. *Nucleic Acids Res*. 1992;20(24):6441-6450.
4. Aasen T, Belmonte JCI. Isolation and cultivation of human keratinocytes from skin or plucked hair for the generation of induced pluripotent stem cells. *Nat Protoc*. 2010;5:371.
5. Ritchie ME, Phipson B, Wu D, et al. limma powers differential expression analyses for RNA-sequencing and microarray studies. *Nucleic Acids Res*. 2015;43(7):e47-e47.
6. Dees C, Akhmetshina A, Zerr P, et al. Platelet-derived serotonin links vascular disease and tissue fibrosis. *J Exp Med*. 2011;208(5):961-972.
7. Schniering J, Benešová M, Brunner M, et al. Visualisation of interstitial lung disease by molecular imaging of integrin αvβ3 and somatostatin receptor 2. *Ann Rheum Dis*. 2019;78(2):218 LP - 227.
8. Chakraborty D, Šumová B, Mallano T, et al. Activation of STAT3 integrates common profibrotic pathways to promote fibroblast activation and tissue fibrosis. *Nat Commun*. 2017;8(1):1130.
9. Hatakeyama M, Opitz L, Russo G, Qi W, Schlapbach R, Rehrauer H. SUSHI: an exquisite recipe for fully documented, reproducible and reusable NGS data analysis. *BMC Bioinformatics*. 2016;17(1):228.
10. Bolger AM, Lohse M, Usadel B. Trimmomatic: a flexible trimmer for Illumina sequence data. *Bioinformatics*. 2014;30(15):2114-2120.
11. Langmead B, Salzberg SL. Fast gapped-read alignment with Bowtie 2. *Nat Methods*. 2012;9(4):357-359.
12. Zhang Y, Liu T, Meyer CA, et al. Model-based Analysis of ChIP-Seq (MACS). *Genome Biol*. 2008;9(9):R137.
13. Robinson MD, McCarthy DJ, Smyth GK. edgeR: a Bioconductor package for differential expression analysis of digital gene expression data. *Bioinformatics*. 2009;26(1):139-140.
14. Li D, Hsu S, Purushotham D, Sears RL, Wang T. WashU Epigenome Browser update 2019. *Nucleic Acids Res*. 2019;47(W1):W158-W165.
15. Dunham I, Kundaje A, Aldred SF, et al. An integrated encyclopedia of DNA elements in the human genome. *Nature*. 2012;489(7414):57-74.
16. Lee CM, Barber GP, Casper J, et al. UCSC Genome Browser enters 20th year. *Nucleic Acids Res*. November 2019.
17. Flicek P, Amode MR, Barrell D, et al. Ensembl 2014. *Nucleic Acids Res*. 2013;42(D1):D749-D755.
18. Fishilevich S, Nudel R, Rappaport N, et al. GeneHancer: genome-wide integration of enhancers and target genes in GeneCards. *Database*. 2017;2017.
19. Wang Y, Song F, Zhang B, et al. The 3D Genome Browser: a web-based browser for visualizing 3D genome organization and long-range chromatin interactions. *Genome Biol*. 2018;19(1):151.
20. Rao SSP, Huntley MH, Durand NC, et al. A 3D Map of the Human Genome at Kilobase Resolution Reveals Principles of Chromatin Looping. *Cell*. 2014;159(7):1665-1680.

Supplementary Figures and Tables

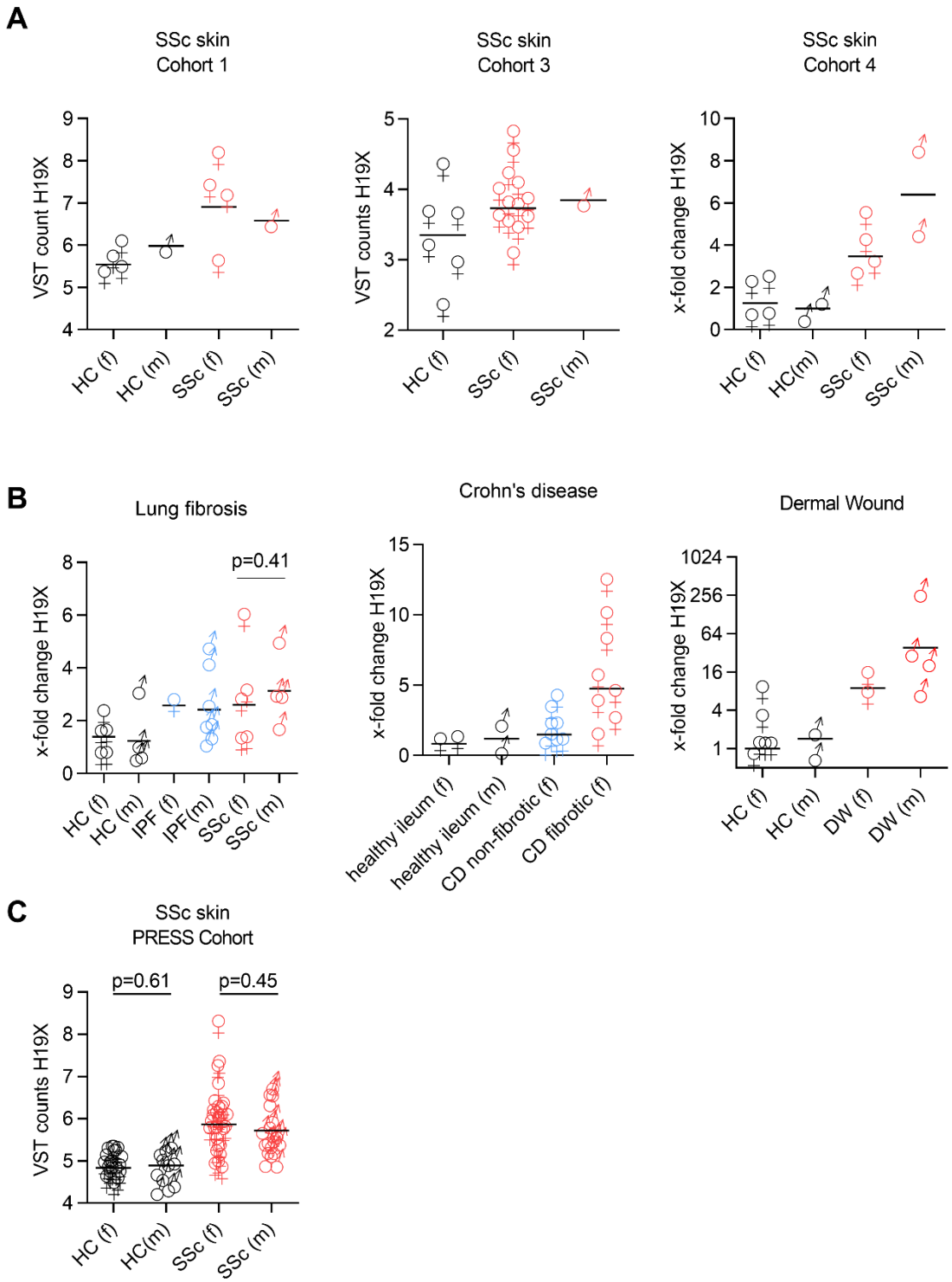

Supplementary Figure 1. H19X differential expression in women and men skin (SSc and HC) in the cohort 1 and cohort 3 as measured by RNA-seq. H19X differential expression as measured by qPCR in cohort 4, normalized to *GAPDH* and *RPLP0* (A). H19X differential expression in women and men in other fibrotic diseases (IPF, SSc-ILD, Crohn's disease) and dermal wounds as measured by qPCR with normalization to *GAPDH* and *RPLP0* (B). H19X differential expression in women and men skin (SSc and HC) in the large PRESS cohort as measured by RNA-seq (C). Data are presented as single values and median. Mann–Whitney test (B, lung fibrosis).

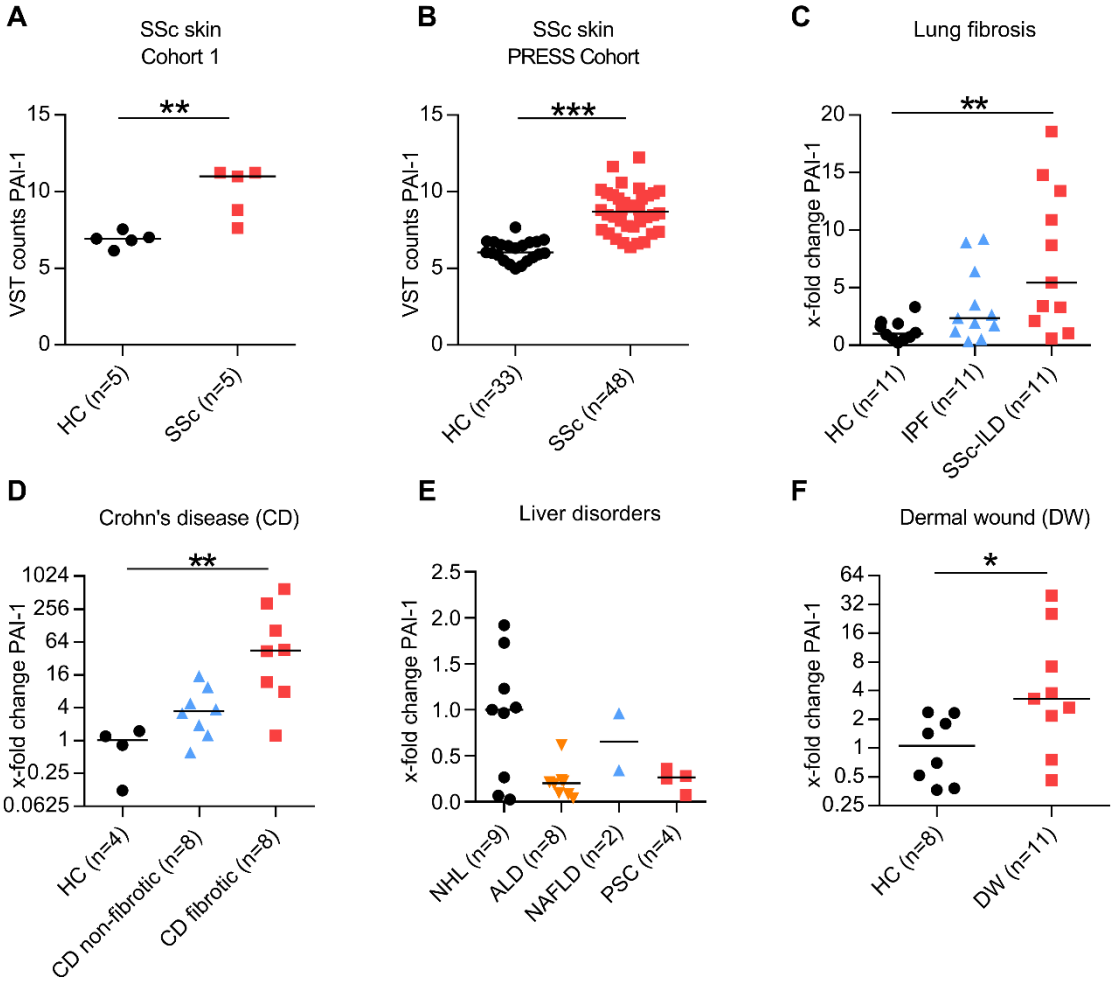

Supplementary Figure 2. PAI-1 differential expression in SSc vs HC skin in cohort 1 (A) and the PRESS cohort (B) as measured by RNA-seq. H19X differential expression in ILD-SSc and IPF (C), Crohn's disease (D), PBC (E), and dermal wound (F) as measured by qPCR and normalized to *GAPDH* and *RPLP0* . Data are presented as single values and median. Differential expression analysis was carried out on variance stabilized counts (VST) using DEseq2 package 44 (A, B). Kruskal–Wallis test (C-E). Mann–Whitney test (F). ** p<0.01, *** p<0.001.

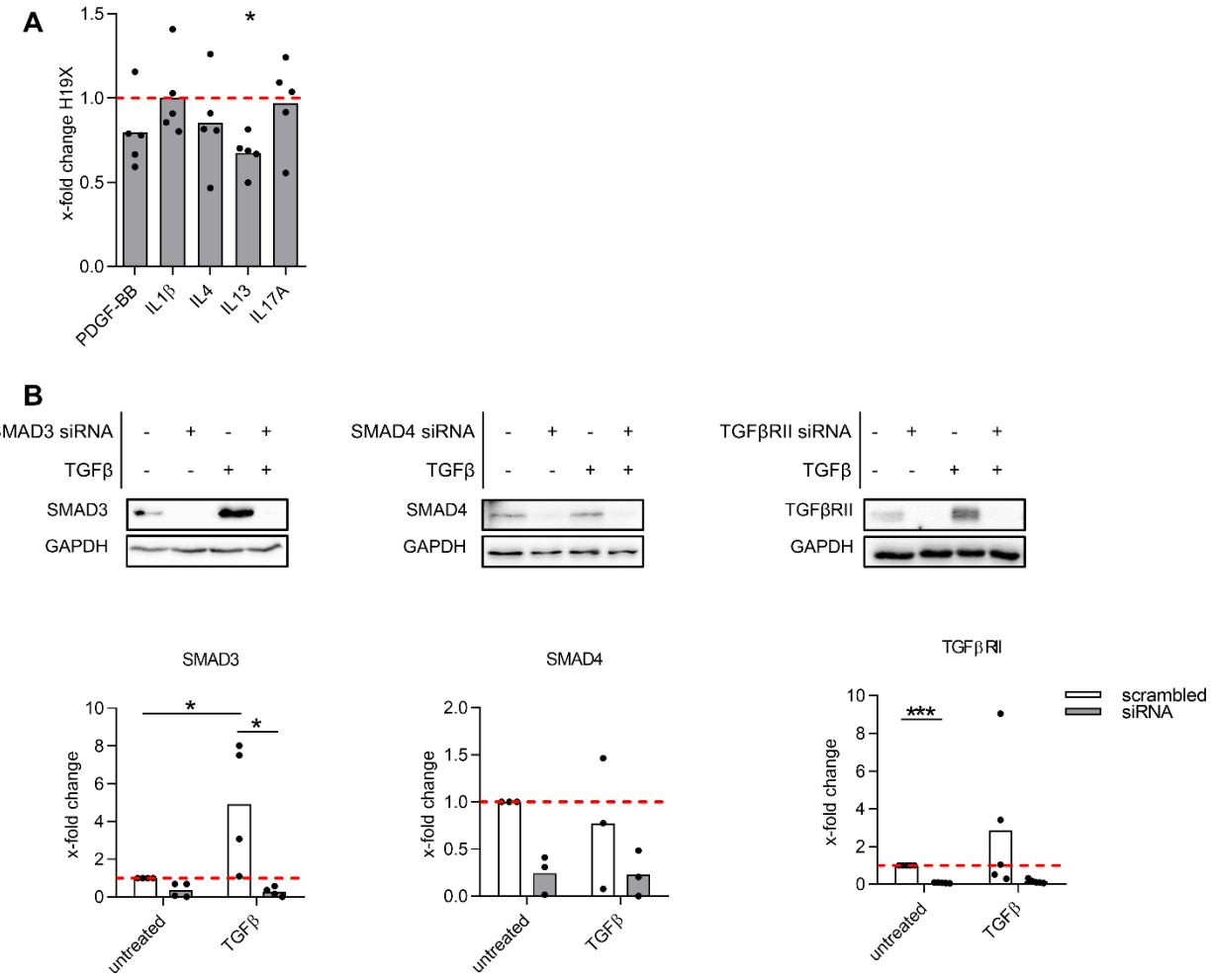

Supplementary Figure 3. SSc fibroblasts were stimulated with PDGF-BB (20ng/ml), IL-1β (10ng/ml), IL-4 (10ng/ml), IL-13 (10ng/ml) or IL-17a (10ng/ml) for 24h. H19X expression was measured by qPCR and normalized to *GAPDH* and *RPLP0* (A). *TGFBR2* and *SMAD*s silencing was performed in SSc fibroblasts with 50nM siRNA for a total of 54h and stimulated with TGFβ for the last 6h in 1% FBS medium. Western blot analysis for SMAD3, SMAD4 and TGFβR2 pictures are representative of n=3-5 biological replicates and corresponding densitometric analysis (B). Fold change was calculated compared to untreated controls set as 1 (dashed line). Data are presented as mean and single of n=3-5 biological replicates. One-way ANOVA (A, B). * $p<0.05$, *** $p<0.001$.

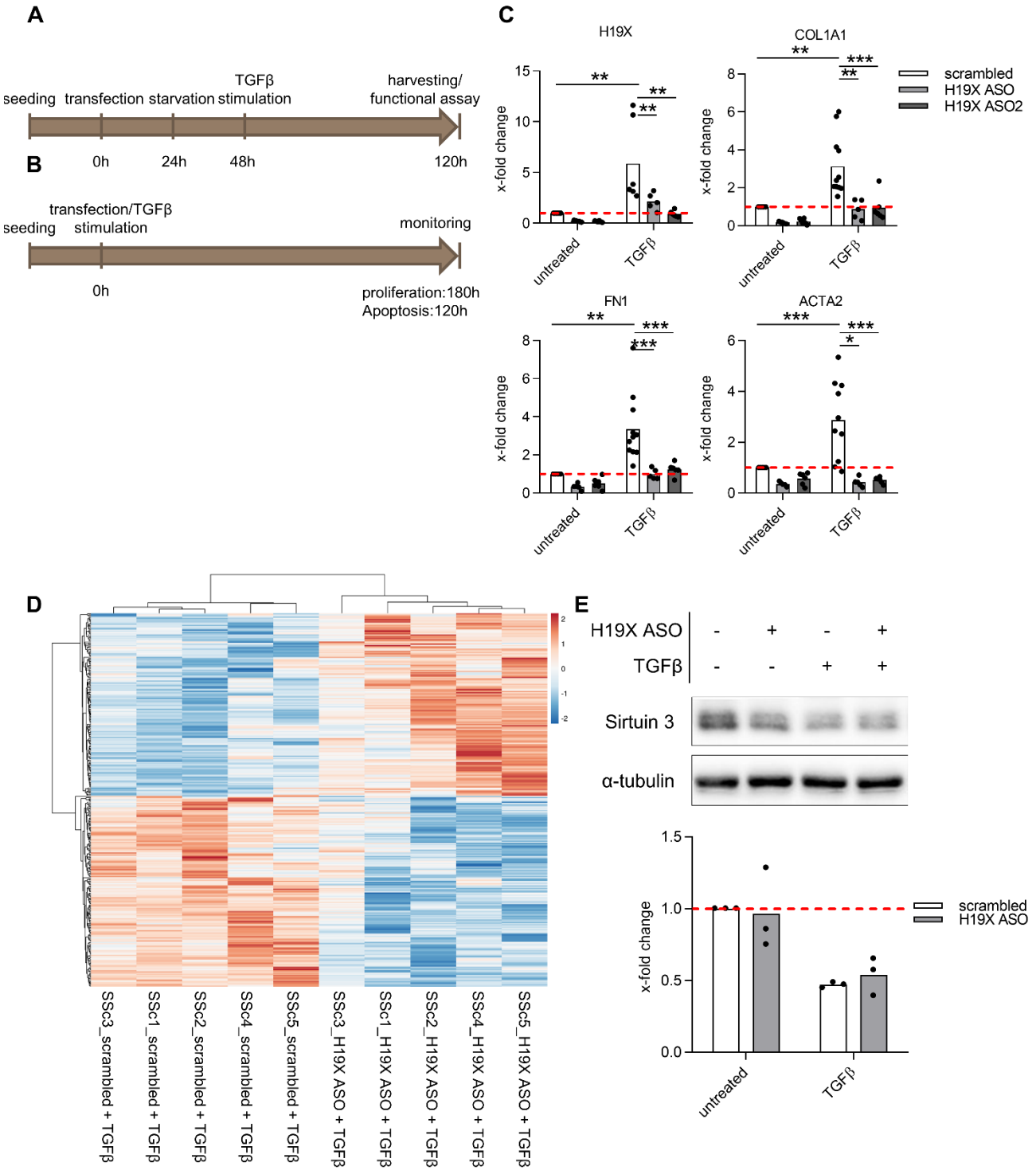

Supplementary Figure 4. Schematic representation of the experimental set-up used to characterize ECM production and myofibroblast activation after H19X silencing (A). Schematic representation of the experimental set-up used to characterize cell cycle and cell apoptosis after H19X silencing (B). H19X silenced was performed with 2 different sets of ASOs (ASO and ASO2). *H19X*, *COL1A1*, *FN1* and *ACTA2* expression was measured by qPCR and normalized to *GAPDH* and *RPLP0*. Fold change was calculated compared to controls set as 1 (dashed line). Data are presented as single values and mean (n=5-6). One-way ANOVA. * p<0.05, ** p<0.01, *** p<0.001 (C). H19X was silenced in dermal SSc fibroblasts with 25nM ASO for a total of 120h and stimulated with TGFβ for the last 72h in 1% FBS medium. Heatmap showing 317 differentially expressed gene identify by microarray experiment at a FDR of <5% and Log2FC >|0.5| and unsupervised hierarchical clustering. Differential expression analysis was carried out using 'limma' R-package (D). Sirtuin-3,protein levels were analyzed by Western blot. Pictures are representative of n=3 biological replicates. The protein level was semi-quantified by densitometric analysis. For Western blot, semi-quantification fold change was calculated compared to controls set as 1 (dashed line) (E).

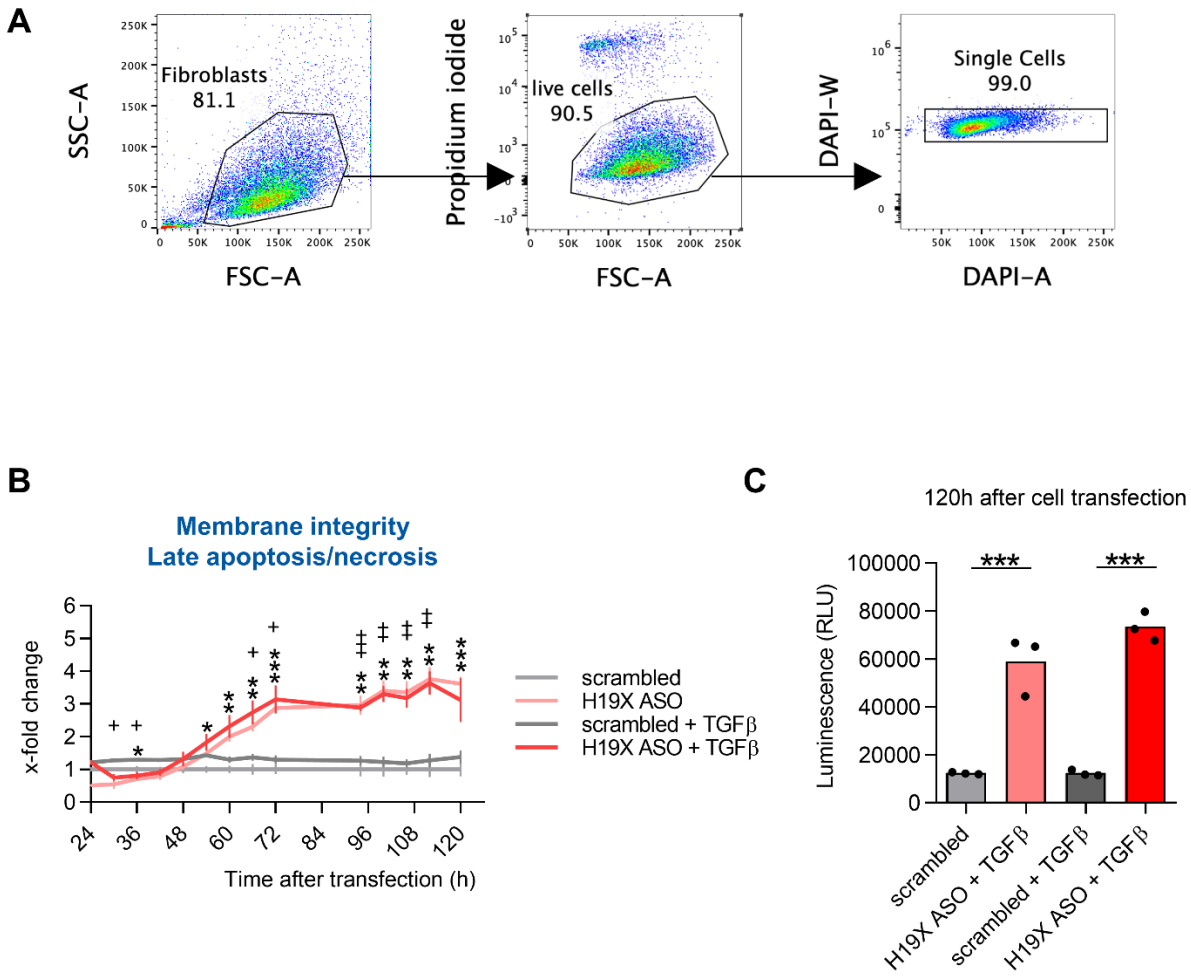

Supplementary Figure 5. H19X was silenced in dermal SSc fibroblasts with 25nM ASO for a total of 120h and stimulated with TGFβ for the last 48h in 1% FBS medium. Cell were stained with Hoechst 33342. Forward and side scattergrams (FSC/SSC) were used to select total cells. Next, living cells were selected as propidium iodide (PI) negative cell population (A). Fluorescence (DNA dye) as a measure of necrosis was recorded every 6h starting 24h until 120h after cell transfection. Fold change was calculated respective to scrambled control. * indicate significance for untreated cells, + indicate significance for TGFβ stimulated cells (B). Caspases 3/7 activity measured at 120h after cell transfection (C). Data are presented as single values and mean (n=3-5). One-way ANOVA (C). Two-way ANOVA (B). * p<0.05, ** p<0.01, *** p<0.001.

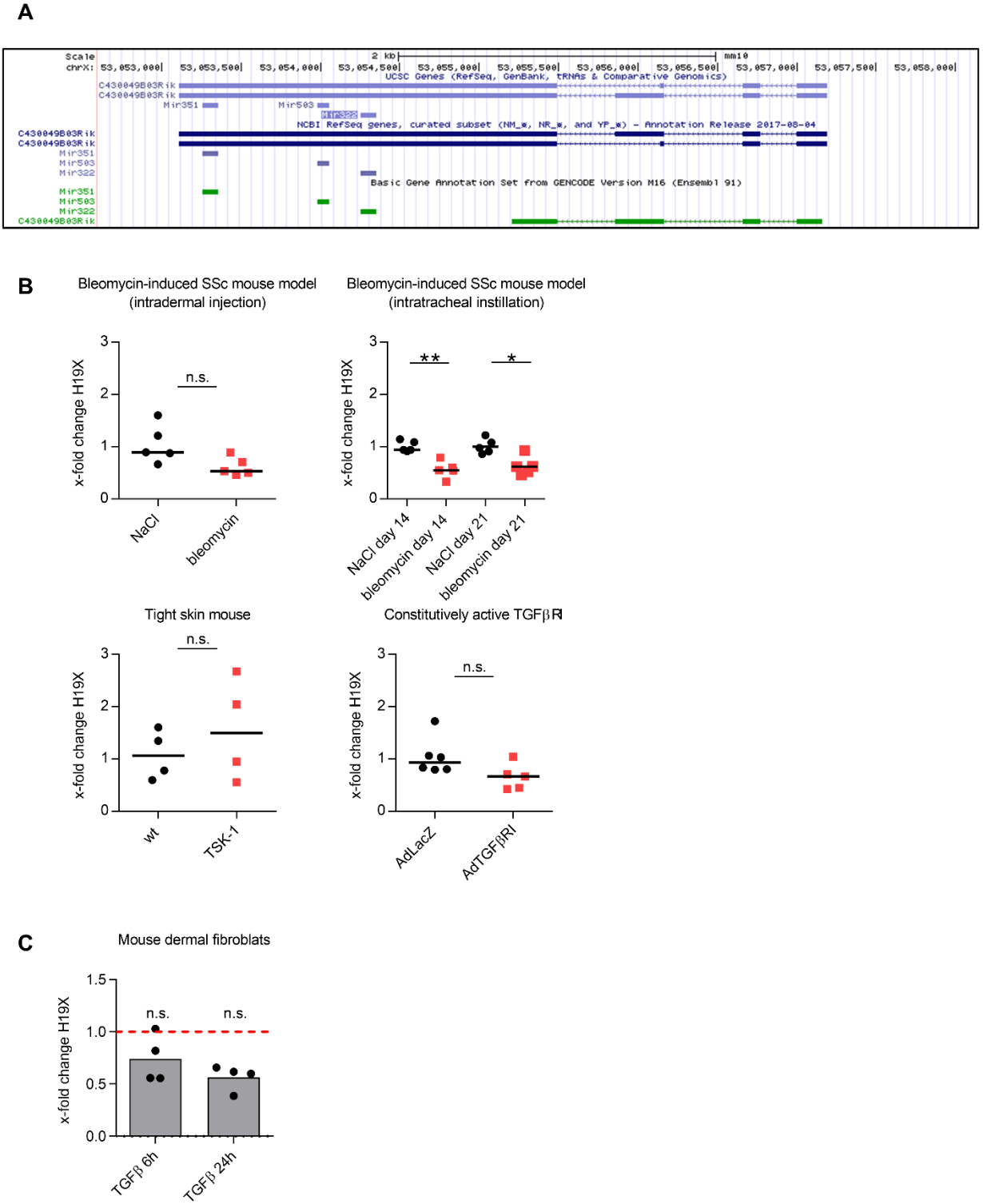

Supplementary Figure 6. Schematic representation of the putative murine H19X (mH19X) locus as annotated in the NCBI Reference Sequence Database (RefSeq, blue) and GENCODE consortium version M16 (green) (A). mH19X expression was measured in 4 established SSc mouse models: bleomycin-induced skin fibrosis (skin), bleomycin-induced lung fibrosis using intratracheal installation (lung), tight skin mouse-1 (skin), injections of adenovirus overexpressing a constitutively active TGFβR1 (skin). H19X expression was measured by qPCR and normalized to *Gapdh*. Data are presented as single values and median (n=4-6). Mann–Whitney test. * $p<0.05$, ** $p<0.01$, n.s., non-significant (B). mH19X was measured in mouse dermal fibroblasts after 6 and 24h of TGFβ stimulation. mH19X expression was measured by qPCR and normalized to *Gapdh*. Fold change was calculated compared to untreated controls set as 1 (dashed line). Data are presented as mean and single values of 4 biological replicates. T-test. n.s., non-significant (C).

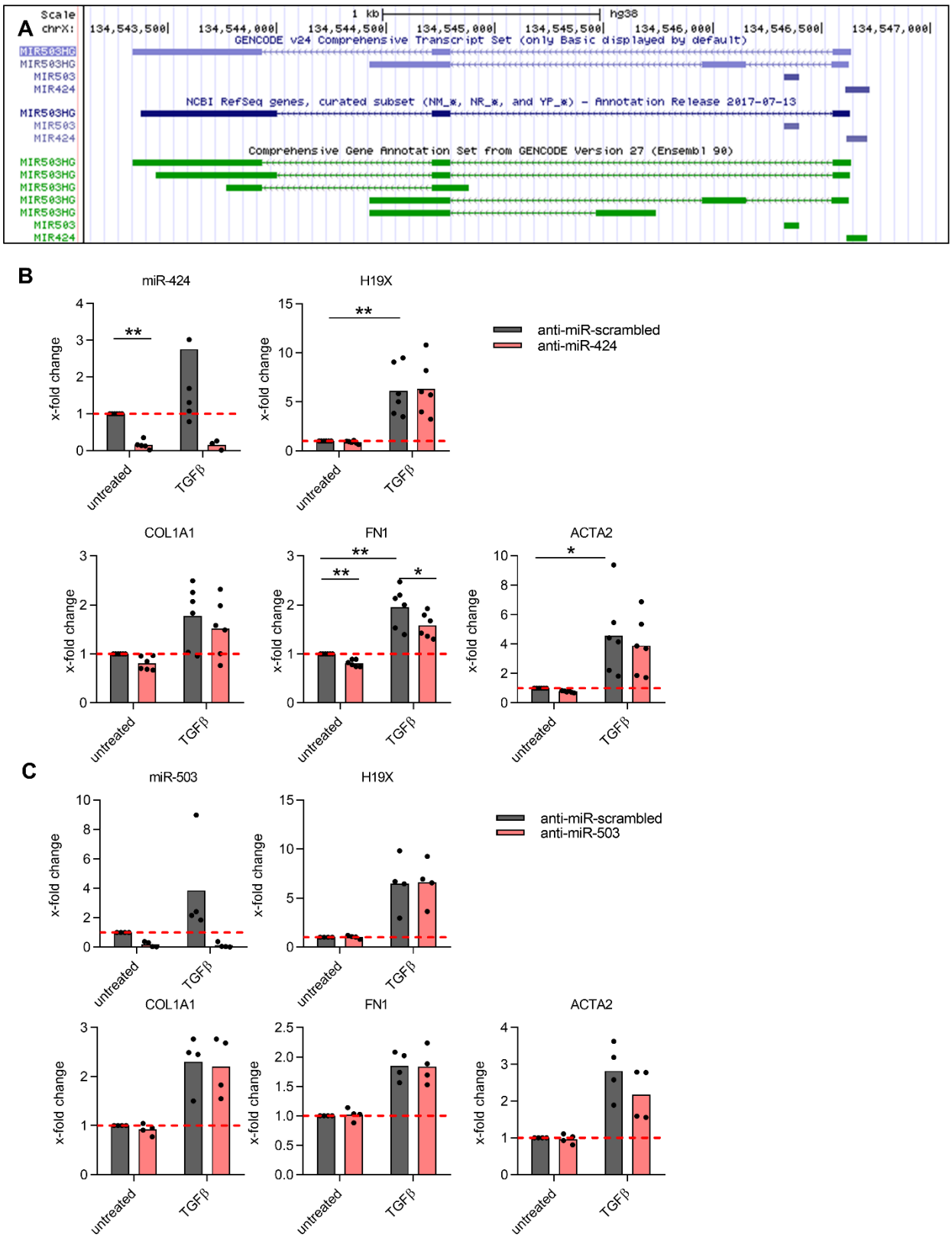

Supplementary Figure 7. LncRNA *H19X* gene is localized on the chromosome X, the same locus encodes also for miR-424 and miR-503 (A). SSc fibroblasts were transfected 100nM of anti-miR-424 or anti-miR-503 for 72h and stimulated for the last 24h with TGFβ in 1% FBS medium (B and C). Expression of miR-424 and miR-503 was analyzed by qPCR and normalized to RNU48. H19X, *COL1A1*, *FN1* and *ACTA2* expression was measured by qPCR and normalized to *GAPDH* and *RPLP0*. Fold change was calculated respective to untreated control set as 1 (dashed line). Data are presented as single values and mean (n=5-6). One-way ANOVA (B, C). * p<0.05, ** p<0.01.

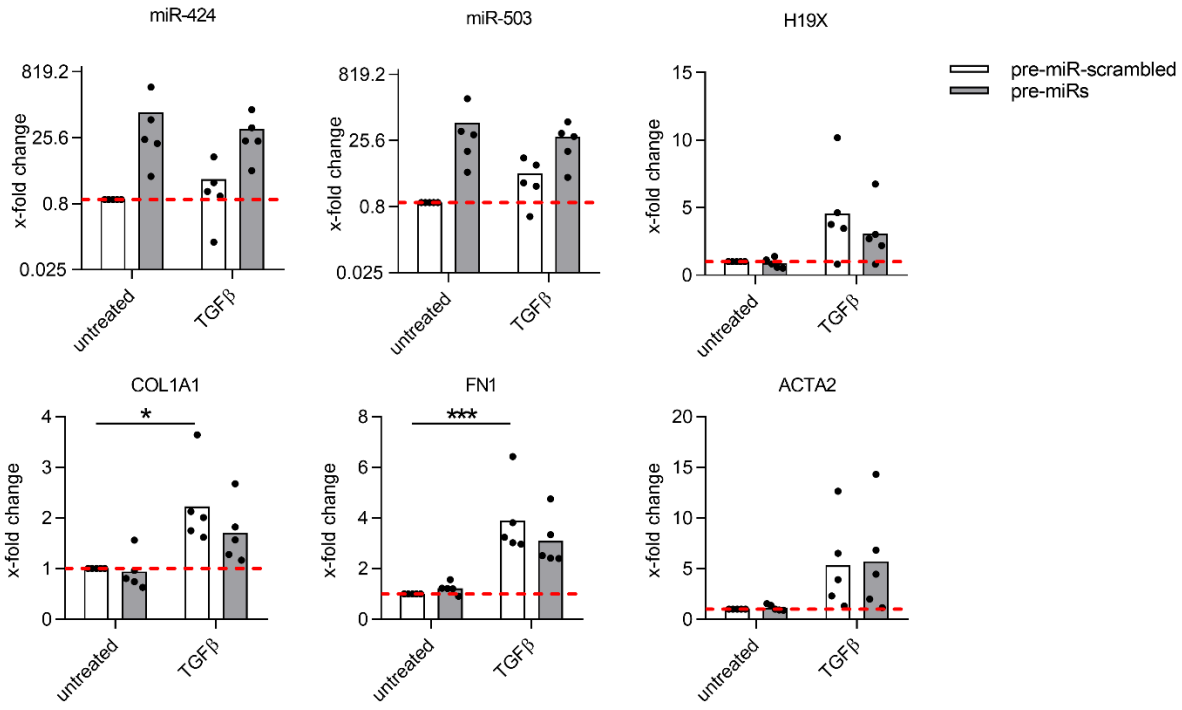

Supplementary Figure 8. SSc fibroblasts were transfected 100nM of pre-miR (miR-424 and miR-503 simultaneously anti-miR-503 for 120h and stimulated for the last 72h with TGFβ in 1% FBS medium). Expression of miR-424 and miR-503 was analyzed by qPCR and normalized to RNU48. H19X, *COL1A1*, *FN1* and *ACTA2* expression was measured by qPCR and normalized to *GAPDH* and *RPLP0*. Fold change was calculated respective to untreated control set as 1 (dashed line Data are presented as single values and mean (n=5). One-way ANOVA. * p<0.05, ** p<0.01.

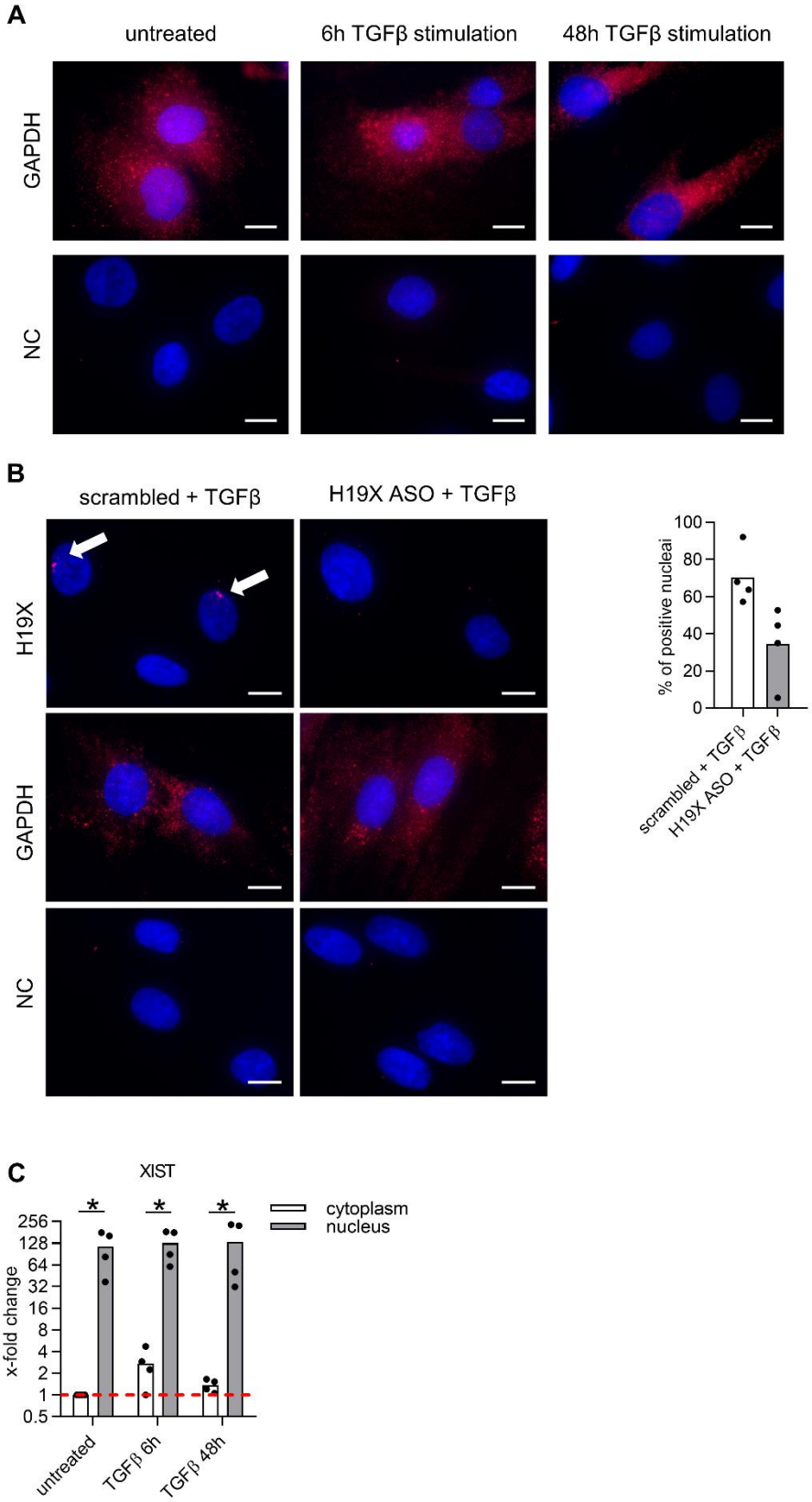

Supplementary Figure 9. SSc fibroblasts were stimulated for 6 or 48h with TGFβ in 1% FBS medium and FISH staining was performed targeting *GAPDH* as positive control. Hybridization buffer without probes was used to assess background signal (NC). Scale: 10µm. Pictures are representative of n=4 biological replicates (A). To verify probe specificity, SSc fibroblasts were transfected with 25nM of ASO targeting H19X for 96h and stimulated for the last 48h with TGFβ in 1% FBS medium. FISH staining was performed targeting H19X and *GAPDH* as positive control. Hybridization buffer without probes

was used to assess background signal (NC). Scale: 10µm. Pictures are representative of n=4 biological replicates. Percentage of nuclei positive for H19X staining (B). Cell fractions were obtained from SSc fibroblasts stimulated with TGFβ for 6 or 48h in 1% FBS. XIST expression was used to evaluate successful cell fractionation (C). Fold change was calculated respective to control (dashed line). Data are presented as mean and single values of n=4 biological replicates. T-test (B) and One-way ANOVA (C). * $p<0.05$; ** $p<0.01$; *** $p<0.001$.

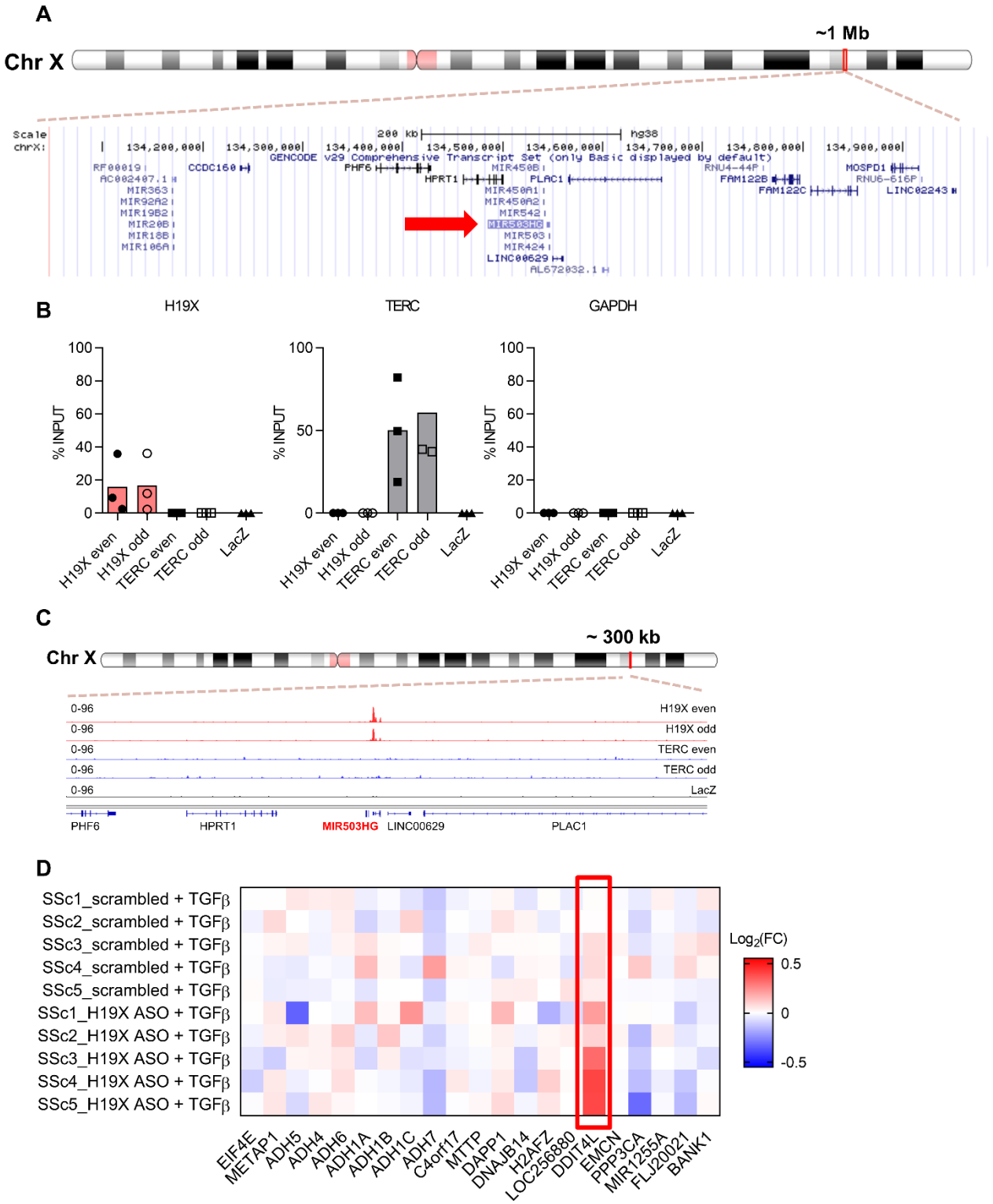

Supplementary Figure 10. Schematic representation of *H19X* (*MIR503HG*) locus and its neighboring genes spanning 1Mb (A). BJ5TA cells were stimulated with TGFβ for 6h in 1% FBS medium. RNA retrieval after ChIRP experiments was assessed by qPCR and shown as % respective to the input. *GAPDH* was used to assess the assay specificity. Data are presented as mean and single value of n=3 independent experiments (B). ChIRP peaks for H19X capture are shown as fold enrichment relative to input for two sets of probes (even, odd, red tracks), TERC probes were used to validate the method. *LacZ* probes were used as negative control. Specific peak at the H19X transcription start site was identified (C). Heatmap showing expression of the gene within the same genomic region of *DDIT4L* (in red) as measured by microarray analysis following H19X silencing (D).

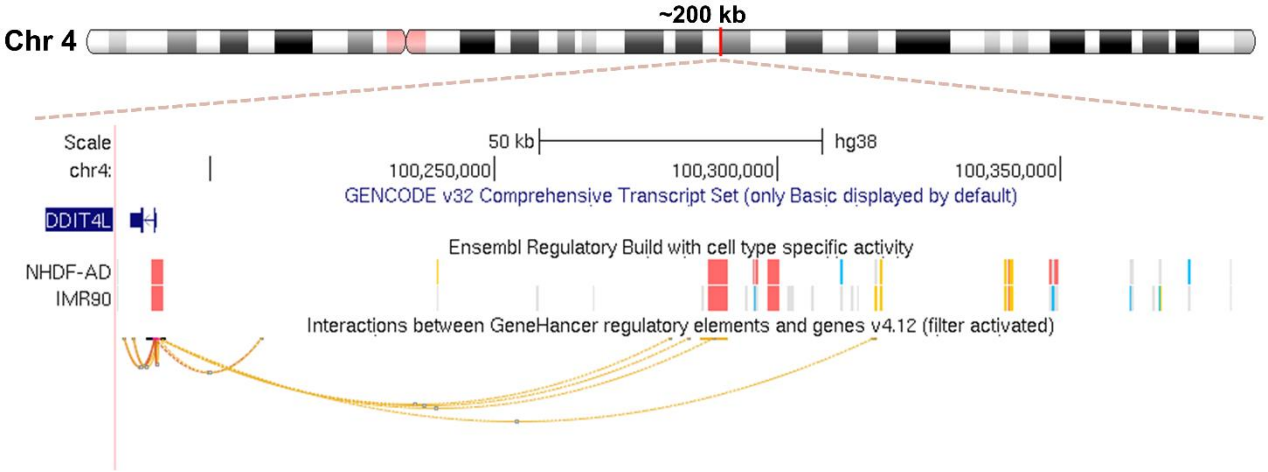

Supplementary Figure 11. GeneHancer results for *DDIT4L* promoter showing interactions with *DDIT4L* enhancer. Ensembl Regulatory Annotation for DNA regulatory elements and activity in IMR90 cell line (fibroblasts) and adult normal human dermal fibroblasts (NHDF-AD), in red predicted active promoter flanking regions, in yellow unannotated active open chromatin regions, in blue active CTCF binding sites, in grey inactive regions.

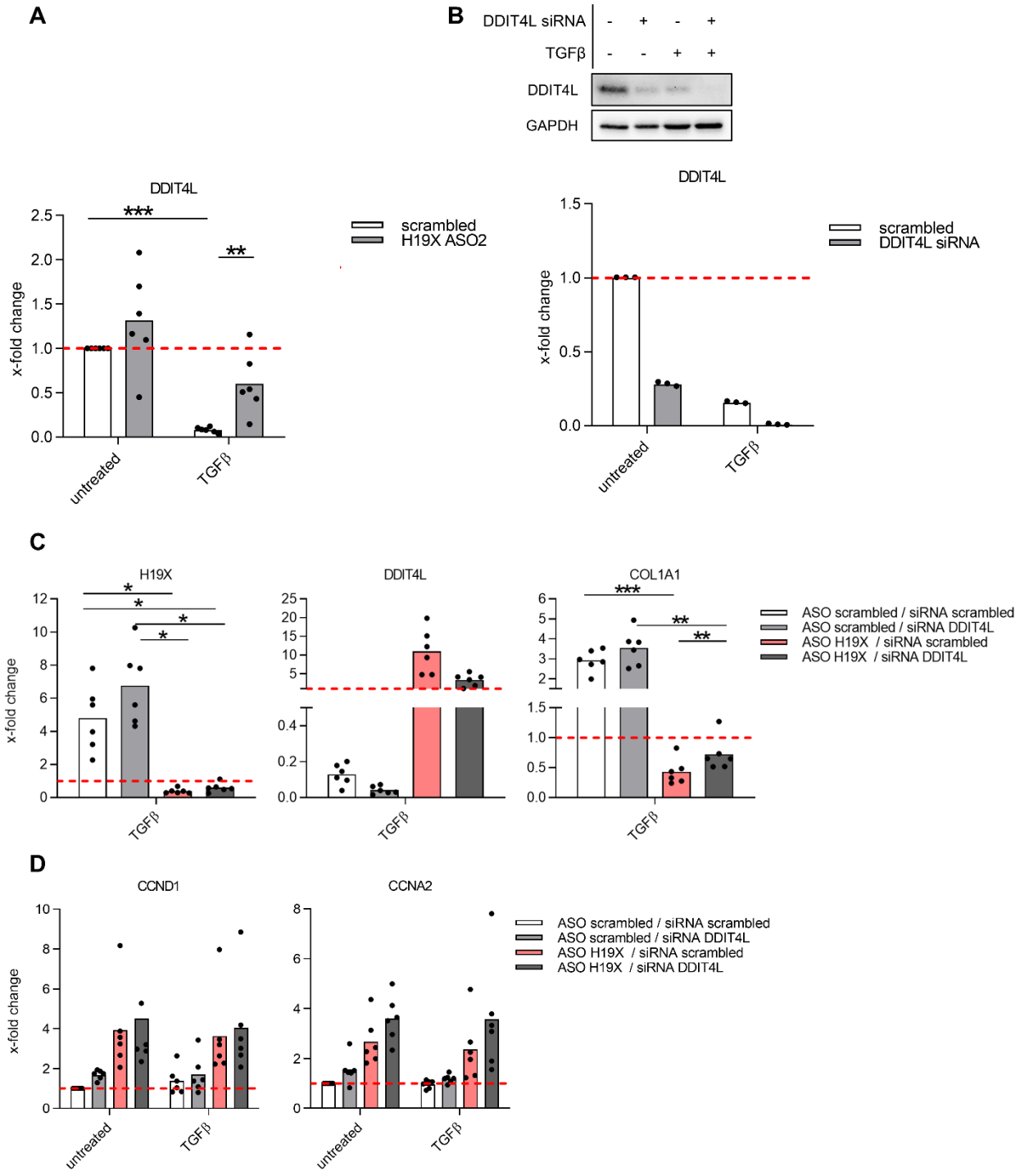

Supplementary Figure 12. H19X was silenced in dermal SSc fibroblasts with 25nM ASO_2 for a total of 120h and stimulated with TGFβ for the last 72h in 1% FBS medium. H19X silenced was performed with a second set of ASO (ASO_2). *DDIT4L* expression was measured by qPCR and normalized to *GAPDH* and *RPLP0*. Data are presented as single values and mean (n=6) (A). *DDIT4L* silencing was performed in SSc fibroblasts with 50nM siRNA for 120h and TGFβ stimulated for the last 72h in 1%FBS medium. Western blot analysis for DDIT4L (pictures are representative of n=3 biological replicates), corresponding densitometric analysis Data are presented as mean and single values (n=3) (B). SSc fibroblasts were transfected with 25nM of ASO and 50nM of siRNA for 120h and stimulated with TGFβ for the last 72h in 1% FBS medium. Expression of H19X, *DDIT4L*, *COL1A1* (TGFβ stimulated samples, C) *CCNA2* and *CCND1* (D) was analyzed by qPCR and normalized to *GAPDH* and *RPLP0*. Data are presented as single values and mean (n=6). Fold change was calculated compared to controls set as 1 (dashed line). One-way ANOVA (A-D). * p<0.05, ** p<0.01, *** p<0.001.

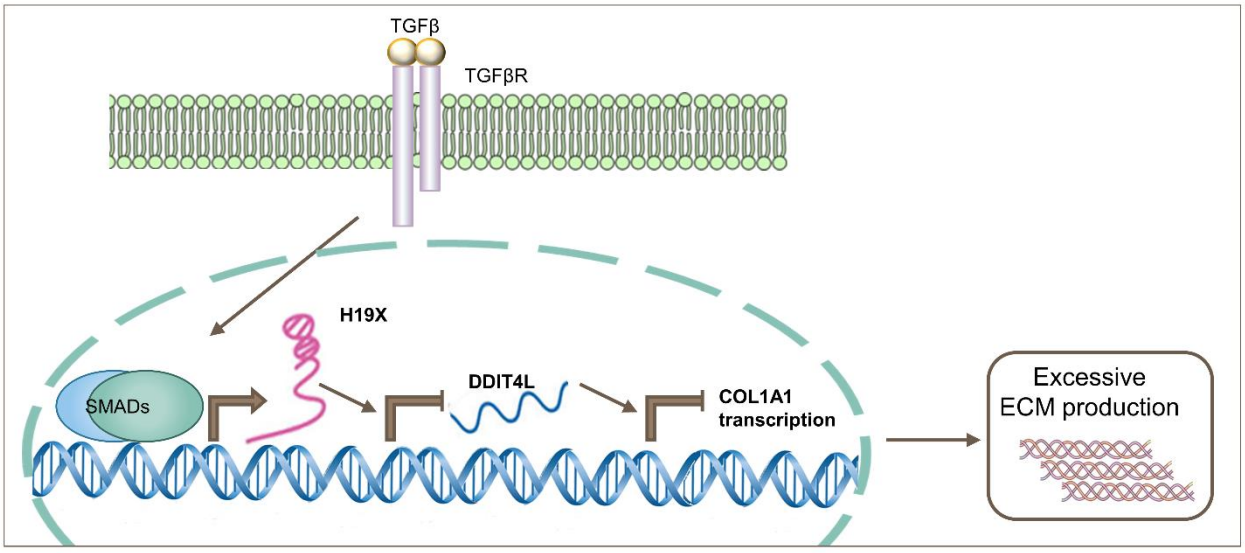

Supplementary Figure 13. Schematic representation of H19X mechanism. TGFβ pathway induces H19X expression which in turn decrease *DDIT4L* expression. The lack of the repressor, DDIT4L, results in enhanced *COL1A1* transcription and therefore in ECM accumulation.

Supplementary Table 1. H19X transcripts coding potential assessment. Coding potential assessment tool (CPAT) was used to calculate coding potential for each transcript variant. Human coding probability (CP) cutoff: 0.364

Transcript ID	*RNA Size (nt)*	*ORF Size (nt)*	*Fickett Score*	*Hexamer Score*	*Coding Probability (CP)*	*Coding Label*
ENST00000440570.5	760	147	0.8435	-0.0335	0.0159	No
ENST00000414769.1	720	138	0.4527	-0.1723	0.0017	No
ENST00000441492.1	649	270	0.5757	0.0833	0.0543	No
ENST00000457876.5	646	117	1.0186	-0.2711	0.0042	No
ENST00000445415.1	332	72	0.7253	-0.3612	0.0006	No
ENST00000440570.5	760	147	0.8435	-0.0335	0.0159	No

Supplementary Table 2. Correlation analysis of H19X expression with TGFβ genes (KEGG Pathway database). Significant correlations are highlighted in pink (Pearson p<0.05). Genes with significant correlations and Pearson correlation coefficients r>|0.5| are marked in red.

TGFβ pathway gene (symbol)	Pearson correlation coefficient (r)	Pearson p-value	TGFβ pathway gene (symbol)	Pearson correlation coefficient (r)	Pearson p-value
TGFBR1	0.746617561	1.86E-15	ACVR1C	0.160573492	0.154776653
GDF6	0.695810054	7.85E-13	PPP2R1A	0.159104039	0.158637155
BMPR2	0.672841557	8.14E-12	BMP2	-0.148052159	0.189988414
TGFBR2	0.617367236	1.07E-09	ACVR2A	-0.147359103	0.192093785
TGFB3	0.557046663	8.04E-08	AMH	0.137265585	0.224680968
THBS1	0.54172736	2.11E-07	DCN	-0.137153235	0.225064244
TGFB1	0.508543099	1.46E-06	ID3	0.133168653	0.238954509
RHOA	0.485290914	5.06E-06	SMAD2	0.130631789	0.248100933
ID4	-0.455383118	2.19E-05	SMURF1	-0.126585936	0.263179558
SMURF2	0.447250816	3.19E-05	SKP1	-0.12155539	0.282776946
INHBA	0.435198604	5.48E-05	TFDP1	0.118255295	0.296146891
ACVR1	0.429929002	6.89E-05	SMAD5	-0.116837389	0.30201673
ROCK1	0.420708595	0.000102049	BMP8B	-0.115351522	0.308248827
SMAD7	0.404661965	0.000196853	RBL1	-0.113808641	0.3148077
BMPR1B	0.398413911	0.000252005	MAPK1	-0.112845802	0.318946026
E2F4	0.382456868	0.000463401	PITX2	0.11089513	0.327436633
BMP6	0.38238945	0.000464565	IFNG	0.107941287	0.3405649
TGIF1	0.331393886	0.002675363	BMP7	-0.100925166	0.373051363
ACVR1B	-0.322317441	0.003548169	CUL1	-0.087066867	0.442514895
PPP2CB	0.298040027	0.007250548	BAMBI	-0.084052182	0.458531736
TGIF2	0.295064794	0.007883	EP300	0.070231431	0.535884946
ID1	-0.292802439	0.008395848	MAPK3	-0.064962042	0.566984149
ACVR2B	-0.291996078	0.008585588	SMAD6	0.06122142	0.589563033
PPP2R1B	0.291513385	0.008700958	MINOS1-NBL1	-0.054859895	0.628866091
SP1	-0.290104122	0.009045597	ZFYVE16	0.050405004	0.657025961
MYC	0.285498903	0.010256545	BMP8A	0.039743059	0.726326355
GDF7	-0.266125434	0.017031116	RBX1	-0.038540392	0.734295935
ID2	-0.256475826	0.0216506	BMP5	0.036519583	0.747750034
ZFYVE9	-0.243313051	0.029644846	CDKN2B	-0.028775212	0.799978371
CHRD	0.240098547	0.031937342	BMP4	-0.019933316	0.860686454
SMAD4	-0.222371242	0.047418415	INHBE	0.009358271	0.934338702
NOG	0.220346276	0.049526531	GDF5	-0.009341298	0.934457527
SMAD3	-0.21575431	0.054593517	SMAD1	0.009279035	0.934893434
BMPR1A	-0.207530629	0.064723646	E2F5	-0.007588082	0.94673882
CREBBP	0.194080121	0.084522365	PPP2CA	-0.00756829	0.946877539
TGFB2	0.184687125	0.100997861	INHBC	-0.006624434	0.953494658
RPS6KB2	-0.182129176	0.10589347	RPS6KB1	-0.002369284	0.983358914
NODAL	-0.181481357	0.107162142	SMAD9	-0.002164486	0.984797173
FST	0.177291328	0.115654975	LEFTY1	-0.001038817	0.992703262
LTBP1	0.171481781	0.128277272	E2F5	-0.007588082	0.94673882
INHBB	-0.163903424	0.146287944	PPP2CA	-0.00756829	0.946877539
AMHR2	-0.162656699	0.149424231	INHBC	-0.006624434	0.953494658

Supplementary Table 3. Correlation analysis of H19X expression with different cell type specific gene signatures Significant correlations are highlighted in pink (Pearson p<0.05). Fibroblast gene signature is marked in red.

Cell type	*Pearson correlation coefficient (r)*	*Pearson p-value*
Fibroblast	**0.5919**	**<.0001**
Hair outer root sheath	**-0.3905**	**0.0027**
Keratinocyte	**-0.3565**	**0.0065**
M2 Macrophage	**0.2983**	**0.0242**
M1 Macrophage	**0.2816**	**0.0338**
Monocyte	**0.2685**	**0.0434**
B cell	0.2571	0.0535
NK cell	0.2527	0.0579
Microvascular endothelial cell	0.2321	0.0823
CD8+ T cell	0.1762	0.1898
Melanocyte	-0.1488	0.2694
CD4+ T cell	0.1349	0.3172
Plasma Cell	0.1096	0.4169
Dendritic cell	0.1091	0.4193
Neutrophil	-0.0008	0.9952

Supplementary Table 4. Expression of genes of the same genomic region (within 1 Mb) as H19X after H19X silencing

Symbol	Description	Location (GENECODE v29)	log2FC (n=5)	adj p-value (n=5)
PLAC1	placenta-specific 1	chrX:134,565,838-134,658,483	0.12	0.69
FAM122B	family with sequence similarity 122B	chrX:134,769,566-134,797,134	-0.04	0.98
FAM122C	family with sequence similarity 122C	chrX:134,807,194-134,854,591	-0.08	0.93
MOSPD1	motile sperm domain containing 1	chrX:134,887,626-134,915,267	0.56	0.54
MIR450B	microRNA 450B	chrX:134,540,185-134,540,262	-0.05	0.92
MIR450A1	microRNA 450A1	chrX:134,540,341-134,540,431	0.38	0.66
MIR450A2	microRNA 450A2	chrX:134,540,508-134,540,607	0.04	0.93
MIR542	microRNA 542	chrX:134,541,341-134,541,437	-0.21	0.86
HPRT1	hypoxanthine phosphoribosyltransferase 1	chrX:134,460,153-134,500,668	0.13	0.96
PHF6	PHD finger protein 6	chrX:134,373,253-134,428,790	0.10	0.89
MIR106A	microRNA 106A	chrX:134,170,198-134,170,278	0.12	0.90
MIR18B	microRNA 18B	chrX:134,170,041-134,170,111	0.17	0.70
MIR20B	microRNA 20B	chrX:134,169,809-134,169,877	-0.04	0.87
MIR19B2	microRNA 19B2	chrX:134,169,671-134,169,766	-0.09	0.81
MIR92A2	microRNA 92A2	chrX:134,169,538-134,169,612	0.08	0.86
MIR363	microRNA 363	chrX:134,169,378-134,169,452	-0.02	0.97

Supplementary Table 5. List of the 71 genomic regions interacting with H19X as detected by ChIRP-seq.

Chromosome	Start	End	Distance to feature	Gene name	Type	Fold enrichment H19X_even	Fold Enrichment H19X_odd
chrX	134542696	134544277	-1259	*MIR542*	short_noncoding	50.81	32.51
chr6	144813806	144814240	-480505	*AL024474.2*	long_noncoding	19.27	18.32
chr2	105395207	105395704	32169	*AC108058.1*	long_noncoding	17.23	10.23
chrX	134544598	134544938	1800	*MIR503*	short_noncoding	16.94	8.08
chrX	134546396	134546823	2	*MIR503*	short_noncoding	15.88	10.07
chr11	5224897	5226135	-258	*CoTC_ribozyme*	short_noncoding	15.35	10.09
chr4	100375876	100376293	-185094	*DDIT4L*	protein_coding	14.29	19.63
chr2	205376600	205377032	-305390	*NRP2*	protein_coding	13.95	10.53
chr8	102687401	102687815	30937	*AP002851.1*	long_noncoding	13.43	20.34
chr2	238860800	238861238	12768	*TWIST2*	protein_coding	13.31	18.22
chr17	38599630	38600049	-1419	*AC006449.1*	long_noncoding	13.12	19.69
chr5	171291533	171291920	17222	*AC091980.2*	protein_coding	12.70	21.94
chr4	107709930	107710403	10522	*PAPSS1*	protein_coding	12.17	6.35
chr2	44337709	44338162	24153	*PREPL*	protein_coding	12.03	20.21
chr3	37621201	37621688	-47988	*RNU7-73P*	short_noncoding	11.65	17.32
chr11	119719778	119720138	9306	*NECTIN1*	protein_coding	11.08	10.08
chr12	124913822	124914940	-1725	*MIR5188*	short_noncoding	10.66	7.81
chr8	38675375	38675761	29480	*AC016813.1*	long_noncoding	10.36	5.59
chr12	71238693	71239027	-120446	*AC025575.2*	long_noncoding	10.06	19.63
chr19	8774543	8774960	-46958	*AC008734.1*	long_noncoding	9.95	6.84
chr6	166322086	166322538	-13638	*PRR18*	protein_coding	9.53	6.89
chr4	79682431	79682723	18670	*LINC02469*	long_noncoding	9.48	8.06
chr16	88521329	88521890	9724	*AC116552.1*	long_noncoding	9.06	23.91
chr10	31663475	31663675	43913	*AL161935.3*	long_noncoding	9.00	12.13
chr22	24550185	24550553	-5318	*SNRPD3*	protein_coding	8.61	13.89
chr1	35535023	35535434	-22450	*NCDN*	protein_coding	7.94	13.86
chr13	20160276	20160676	773	*GJA3*	protein_coding	7.94	8.47
chr1	107378301	107378694	238294	*NTNG1*	protein_coding	7.94	14.44
chr5	129649136	129649348	-98943	*KIAA1024L*	protein_coding	7.70	11.55
chr5	178564904	178565309	25651	*COL23A1*	protein_coding	7.48	13.46
chr6	155107852	155108182	148872	*AL596202.1*	long_noncoding	7.41	13.86
chrX	78103858	78104294	35848	*TAF9B*	protein_coding	7.38	9.00
chr6	170067112	170067432	-95405	*AL596442.1*	long_noncoding	7.37	6.35
chr20	23088706	23089023	-2366	*CD93*	protein_coding	7.29	11.69
chr7	102525668	102526091	-7887	*RASA4B*	protein_coding	7.04	15.06
chr9	61549528	61549732	-66348	*AL935212.2*	long_noncoding	6.98	11.50
chr13	102744748	102745132	1758	*LINC00283*	long_noncoding	6.97	10.53
chr5	135176920	135177190	-45671	*AC008406.1*	long_noncoding	6.88	9.24
chr8	26315481	26315741	23990	*PPP2R2A*	protein_coding	6.88	6.35
chr10	31692452	31692857	14936	*AL161935.3*	long_noncoding	6.79	5.88

chr12	42433907	42434243	-20813	*Y_RNA*	short_noncoding	6.73	14.30
chr2	180313725	180314057	-306612	*CWC22*	protein_coding	6.66	11.22
chr17	28505123	28505455	-1120	*FOXN1*	protein_coding	6.63	9.77
chr7	102624760	102625133	-8003	*RASA4*	protein_coding	6.63	16.00
chr17	7548656	7549132	-443	*TNFSF12-TNFSF13*	protein_coding	6.56	5.04
chr9	129649118	129649552	-6949	*ASB6*	protein_coding	6.54	14.13
chr2	159574954	159575259	-38608	*Y_RNA*	short_noncoding	6.35	5.77
chr3	87086778	87087111	-2351	*LINC00506*	long_noncoding	6.35	13.28
chr13	96649955	96650417	222726	*MIR4501*	short_noncoding	6.35	13.86
chr11	27259476	27259794	-39363	*BBOX1-AS1*	long_noncoding	6.25	7.33
chr12	48800332	48800665	-9579	*Y_RNA*	short_noncoding	6.08	14.63
chr20	23145264	23145536	-2822	*AL118508.3*	protein_coding	6.03	5.41
chr19	8391299	8391685	-614	*RAB11B-AS1*	long_noncoding	6.02	15.91
chr12	132380712	132380975	17902	*AC148477.9*	protein_coding	6.01	10.73
chr7	109443752	109444183	-117437	*AC002386.1*	long_noncoding	5.82	10.97
chr6	38109373	38109791	-97901	*SNORD45*	short_noncoding	5.72	10.09
chr8	103283204	103283431	-15229	*FZD6*	protein_coding	5.33	4.60
chr2	127515848	127516033	11038	*IWS1*	protein_coding	5.29	8.08
chr18	59585509	59585711	21800	*AC090213.1*	long_noncoding	5.29	8.66
chr1	207464805	207465221	10575	*CR2*	protein_coding	5.29	15.01
chr1	208239727	208240119	4593	*PLXNA2*	protein_coding	5.17	12.50
chr2	109959574	109959927	22136	*AC013268.5*	long_noncoding	5.12	5.49
chr11	34908905	34909175	-6924	*PDHX*	protein_coding	4.94	6.44
chr10	124449504	124449831	680	*NKX1-2*	protein_coding	4.86	9.68
chr9	66817875	66818237	-38551	*ZNF658*	protein_coding	4.76	9.82
chr8	32922873	32923180	-11275	*RNU6-663P*	short_noncoding	4.76	13.28
chr11	104975864	104976038	-6428	*CASP4*	protein_coding	4.76	7.51
chrX	96383816	96384032	26966	*RN7SKP194*	short_noncoding	4.76	5.20
chr2	199017711	199017925	54080	*AC020718.1*	long_noncoding	4.76	8.08
chr3	73614870	73615262	-6843	*PDZRN3-AS1*	long_noncoding	4.60	18.46
chr18	47722278	47722569	-144561	*AC120349.3*	protein_coding	4.23	12.13

Supplementary Table 6. Oligonucleotide list.

Target	*Target Sequence (5'→3')*	*Product type*	*Assay ID*
H19X	AAAGACCAAGCCCGCG	ASO	340612-2
	TTATTTACACGATCC	ASO	362822-1
	AATCATCTCTCAAAGG	ASO	362843-1
Scrambled ASO	GCGTATAGACGTGTT	ASO	300610
SMAD3	ATCAAGGGATTTCCTATGGAA	siRNA	SI00082481
	AAGAGATTCGAATGACGGTAA	siRNA	SI00082495
	AAGGAGCACCTTGACAGATT	siRNA	SI00082502
	AGCCTATACTTTGGCAGGTTA	siRNA	SI05062645
SMAD4	AAGCAGCGTCACTCTACCTAA	siRNA	SI00076020
	CCCTGTTAAACAGTAGTTGTA	siRNA	SI00076041
	AGCAAGGTTGCACATAGGCAA	siRNA	SI03042508
	CTCCAGCTCCTAGACGAAGTA	siRNA	SI03089527
TGFBR2	TCGGTTAATAACGACATGATA	siRNA	SI02223186
	AAAGCCTGGTGAGACTTTCTT	siRNA	SI00301910
DDIT4L	*CAGTGATTGAAGGGTCCTAAA*	*siRNA*	*SI4334974*
	AACCTCAACGAGGTAATATTT	siRNA	SI4180337
	CACCGTCCAGATAACCATGCA	siRNA	SI4158182
	CACGTGAACTTGGAAATTGAA	siRNA	SI00360801
scrambled siRNA	AATCTCCGAACGTGTCACGT	siRNA	1027310

Target	*Product type*	*Assay ID*
miR-424	Pre-miR miRNA Precursor	PM10306
	Anti-miR miRNA Inhibitor	AM10306
miR-503	Pre-miR miRNA Precursor	PM10378
	Anti-miR miRNA Inhibitor	AM10378
scrambled	Pre-miR miRNA Precursor Negative Control	AM17110
	Anti-miR miRNA Inhibitor Negative Control	AM17010

Supplementary Table 7. Primer list

Target	*Forward primer (5'→3')*	*Reverse primer (5'→3')*
H19X	GGTGCCAGCCAGCCTTC	CGTCCACTGGAGGAAGCC
SERPINE1/PAI-1	CAAGATTGATGACAAGGGCATG	TCTGTGGTGCTGATCTCATC
ACTA2	ACAGAGTATTTGCGCTCCG	CCGACCGAATGCAGAAGGA
COL1A1	CAGCCGCTTCACCTACAGC	TTTTGTATTCAATCACTGTCTTGCC
FN1	GGAGAATTCAAGTGTGACCCTCATG	TGCCACTGTTCTCCTACGTGG
XIST	TAGTCATCACAACAGCAGTTCTTT	CTTCAATGGGATCAGTATTCTAAAG
DDIT4L	CTGCTAAGTGATTTTGACTACTG	GCT TTGATTTGGACAGACAGTT
GAPDH	GGGAAGCTTGTCATCAATGGA	TCTCGCTCCTGGAAGATGGT
RPLP0	ACACTGGTCTCGGACCTGAGAA	AGCTGCACATCACTCAGAATTTCA

Supplementary Table 8. FISH and ChIRP-seq probe lists.

Stellaris H19X FISH probe set 1 (5'→3')	***Stellaris H19X FISH probe set 2 (5'→3')***
GTCCGGCAGACCCCACCT	GCTCAATTTCGATGCATC
ACCTGGTGGCAGGAACAC	TCAGGGGGCTGTGTGGAC
TACCTGCTCCTGAGCCGG	CAGAAAAGGGCATCACGC
GGGTGGTATTCTGATTGG	GGTACAAGGAATGTTTTA
GGTTTTCTTCGTTGTCCT	GGCACACTGCAACTTGGA
CGTGGGTGGGGACTGAAG	CATTTTTGTCCTTGGAGG
TTACTCCTTTTCCAGTCC	GAGATGCTGGATGCCTTC
AGACTTCTTGCAGCTGCT	CCGCCAACAGTGTTGATG
CAGGAACCGCAGAGAGGT	GGAGTCTTCTGTGTCCAG
CAGGACATGAGCGCGTTT	ACAGCCTTTGAGAGATGA
GCACATCCTCATTCTGGA	TGGGTGGTTTTCAATGCC
GGCGCAAAGCAGCTAGAA	ACCCTTCTATTTGGGACA
GCAGATTTTTGGGGGAGG	GGAGAGGATTCCTTGGAC
CGCCGGGTTGGAATTGTG	GCGGGGGGAAAGAAATGG
GGGGCGACAAAGGAGTCT	GAAGTGTGGGTATGGGGG
AATCGACAGCTCAGGTCC	CTGACTCATTTGGCGGGA
AAGTCACGAAGGGCTCCT	TCAGTTGAGGTTCCCATC
AACAGTGCCCAGGACTTT	TTTCTGTGACCCTGGTTA
CGACAGTTGTGCAGCACT	CAGAGTTGTGACCACTGC
GGGATGGAGGTGGCTTTA	CTTGTCTGTGTGCATGCA
GAAGGCTCAGGAGGCCAG	TGTGGGGTTCCACTTTAG
TCTTTCAGGAAGGCTGGC	ACAGAGTTGTGACCACTG
CACTGGAGGAAGCCGGAT	CTGTGTGCATGCATACAT
AACCGGTTCCGTGTCTCA	GGTTCCACTTTAGTTCTT
AACCGGTCAGGATCCCTG	CCCACTGTTTTCCTGTGT
CAAGTCAGGATCCCTTGC	
TTGGATTCCGGGAGGCAA	
GGAGACCCGGGCAAAAGG	

ChIRP H19X biotinylated probe set ODD (5'→3')	***ChIRP H19X biotinylated probe set EVEN (5'→3')***
AACACGCGTCCGGCAGAC	ACCTGGTGGCAGGAACAC
CTTCCTTCTGCTCCTGAG	TCTTTCAGGAAGGCTGGC
CACTGGAGGAAGCCGGAT	GAGATGCTGGATGCCTTC
CCGCCAACAGTGTTGATG	GGAGTCTTCTGTGTCCAG
TGGGTGGTTTTCAATGCC	TGCCAATTGGAACAAAGA
TGGGTATGGGGGAACAGC	TTTTCCAAGTAACATTGA
GACCCTGGTTATTGACAT	TTTTCCAAGTAACATTGA
GGGGTTCCACTTTAGTTC	TGTGACCACTGCCTTTTT
GTTGCCCATATTAACGGA	GTCATTCAATGTCCCAGC